PCCP

A Generalized van der Waals Model for Light Gas Adsorption Prediction in IRMOFs

Journal:	*Physical Chemistry Chemical Physics*
Manuscript ID	CP-ART-01-2019-000285.R1
Article Type:	Paper
Date Submitted by the Author:	27-Feb-2019
Complete List of Authors:	Kong, Lingli; University of Wyoming, Department of Chemical Engineering Adidharma, Hertanto; University of Wyoming, Department of Chemical Engineering, Department of Petroleum Engineering

Physical Chemistry Chemical Physics

ARTICLE

A Generalized van der Waals Model for Light Gas Adsorption Prediction in IRMOFs

Lingli Kong[a] and Hertanto Adidharma*[a]

Received 00th January 20xx,
Accepted 00th January 20xx

DOI: 10.1039/x0xx00000x

www.rsc.org/

By making reasonable simplification to the structures of isoreticular metal-organic frameworks (IRMOFs) and defining important attractive regions of square-well potential, an adsorption model derived from the Generalized van der Waals partition function is proposed to describe the isotherms of light gas adsorption in IRMOFs. The simplification of the structures is based on the geometries of the accessible surfaces and the dimensions of the frameworks, and the locations of the attractive regions are defined by examining the distribution of the adsorbate molecules. Grand Canonical Monte Carlo (GCMC) simulation using the simplified structures with square-well potentials and the complete atomic structures with Lennard-Jones potentials and Coulombic potentials are performed and compared to verify the reliability of the simplification. The adsorption model proposed in this work can predict adsorption isotherms of IRMOFs accurately by calculating the adsorbed amounts in different attractive regions of the simplified frameworks. It is also demonstrated that the model with the five parameters fitted to the adsorption isotherm at one temperature can accurately predict the isotherms at other temperatures.

1. Introduction

Metal Organic Frameworks (MOFs) are highly porous materials with crystal structures. Due to their high storage capacity, selectivity ability, and thermal stability, MOFs are widely used for gas storage, gas separation, catalysis, and gas purification.[1] Thus, obtaining the adsorption isotherms of different adsorbates, which contain important equilibrium information,[2] is a crucial step to screen the best MOFs for different purposes. Experiments can always be performed to obtain isotherms, but they are usually costly and time consuming, and therefore experimental efforts should be minimized, and tools, such as molecular simulations and theoretical or engineering models, are commonly used to generate or predict isotherms.

Molecular simulation has been proven to be a powerful tool for characterizing MOFs.[3] Not only can it conduct the calculations and predictions based on the existing MOFs, but it also offers scientists a tool to gain insight into the hypothetical MOFs. GCMC simulation is commonly used for generating adsorption isotherms of MOFs.[4] However, if the complete atomic structures are used, this method highly relies on force fields to obtain the parameters of the frameworks. The standard organic force fields (e.g., the universal force field (UFF)[5] and Dreiding[6]), which have been applied for conducting simulations, do not have universality for this capricious group of materials.[7] With high accuracy in representing the interaction potentials, the second order Møller-Plesset perturbation theory (MP2) and density function theory (DFT) are commonly applied to study the adsorption phenomena in MOFs, [8-10] including MOFs with open-sites.[11, 12] However, *ab initio* method is too expensive to be applied to large systems.[13] Furthermore, it is a time-consuming process to conduct millions of cycles to generate one point on the isotherms, not to mention the time and the computation cost to screen thousands of millions of possible MOFs, and strategies developed for large-scale screening of MOFs are still based on large-scale simulations to build database.[14-18] Considering that the adsorbents used in simulations are rather ideal in structure conformations and purities, parameters obtained theoretically will also be less accurate in dealing with real MOFs, which have various structure defects.

Building simple but accurate models is one of the most desirable tools for predicting adsorption isotherms. However, the application of this idea to MOFs is still far from satisfactory. It was suggested that heat of adsorption, surface area, and free volume are different leading factors for the adsorption in IRMOFs depending on the adsorption regimes at different pressure ranges.[19, 20] The existing adsorption models that have been applied to predict the adsorption phenomena in various MOFs, such as Langmuir adsorption model, Tóth equation, Dubinin-Astakhov (DA) equation, Dubinin-Radushkevich (DR) model, Freundlich equation, and the modified versions of them, are either based on multilayer mechanism, which is dependent on surface area only, or pore-filling mechanism, which is dependent on free volume only.[21] Therefore, the good performance of these models cannot be guaranteed for different MOFs under different adsorption conditions. Multisite Langmuir model, which can take into account the effects of each selected adsorption site on the adsorption isotherms, is

[a] *Department of Chemical Engineering, University of Wyoming, Laramie, Wyoming, 82071-3295, USA. E-mail: adidharm@uwyo.edu*

† Electronic supplementary information (ESI) available: The simplified structure and the distribution of attractive regions.

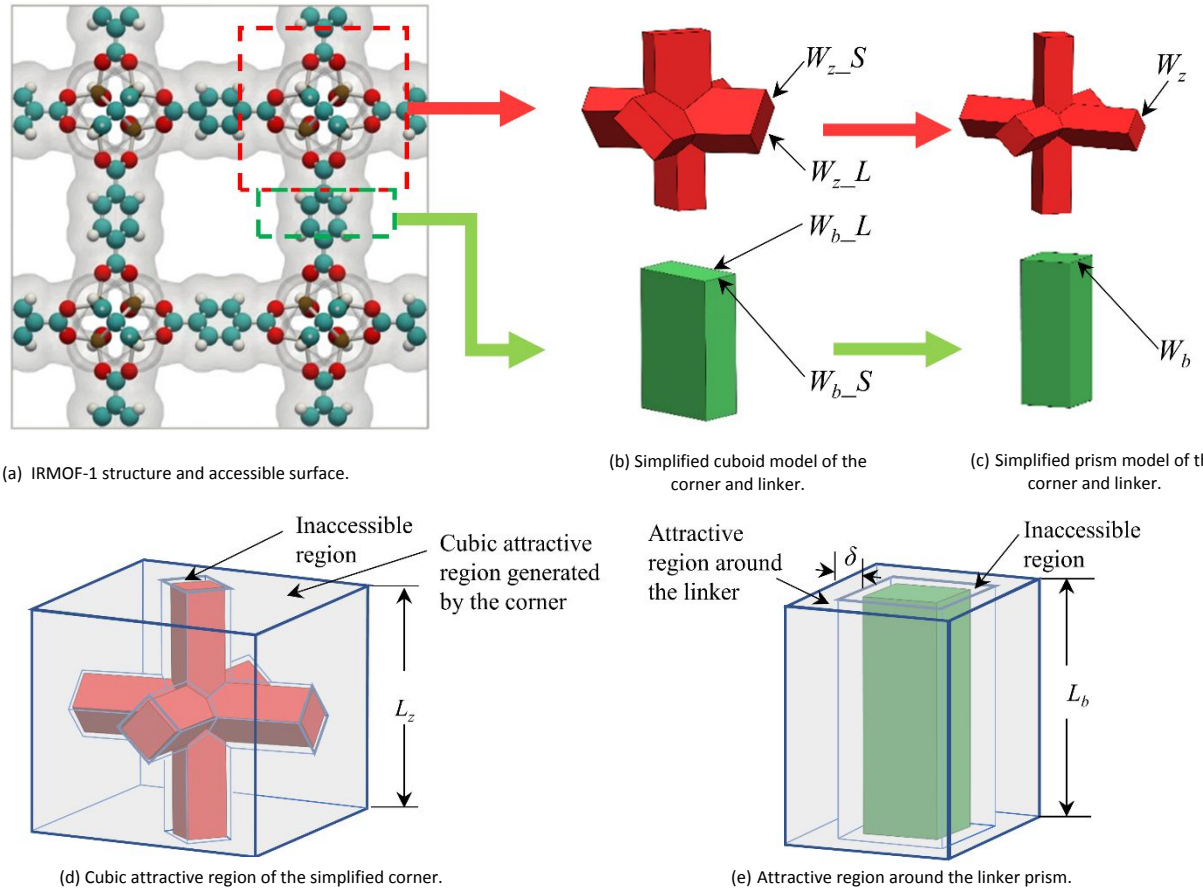

(a) IRMOF-1 structure and accessible surface.

(b) Simplified cuboid model of the corner and linker.

(c) Simplified prism model of the corner and linker.

(d) Cubic attractive region of the simplified corner.

(e) Attractive region around the linker prism.

Red spheres represent oxygen (O) atoms, turquoise spheres represent carbon (C) atoms, white spheres represent hydrogen (H) atoms, and brown spheres represent zinc (Zn) atoms.

Fig. 1 Simplified structure and attractive regions of IRMOF-1

considered to be more realistic because it considers the conformations of the real MOFs, but the calculations of the interaction energy terms still rely on *ab initio* method, which means that the model is computationally expensive. [22,23]

Researchers have also developed engineering models specifically for the adsorption prediction in MOFs. The Sanchez-Lacombe (SL) Equation of State (EOS) and Perturbed Hard Sphere Chain (PHSC) EOS were applied to predict the isotherms by calculating the adsorbate 'solubility' in MOFs.[24-26] This type of model is simple in parameters, but it sacrifices the accuracy. A semiclassical SAFT-VR-2D model was built for the adsorption of a binary mixture of hydrogen and methane in MOFs.[27] However, the model considers MOFs as structureless systems and the influence of the metal clusters and the organic ligands is ignored.

Since MOFs are materials of great variance in structure topologies and building blocks, as the first step toward the modeling of MOFs, we choose to model the adsorption in IRMOFs, which have the same cubic topology with different pore functionalities and sizes.[28] Since the functional groups, such as -Br (IRMOF-2), $-NH_2$ (IRMOF-3), $-OC_5H_{11}$ (IRMOF-5), etc. can lead to chemisorption and dramatically influence the adsorbed amount of some certain gases, we do not discuss this type of IRMOFs. In this work, we propose an adsorption model that considers atoms in different parts of the structure as different groups that can generate attractive regions of square well potential. The adsorbed amount can be obtained by predicting the density of the adsorbate in each attractive region independently. Square-well potential is applied to the adsorbate/adsorbate and adsorbate/adsorbent interactions, which is achieved by implementing structure simplifications.

Considering that there is not enough experimental data available for the adsorption of different gases in different IRMOFs, we use RASPA 2.0[29] to generate adsorption isotherms of IRMOFs as realistic references for testing the reliability of the simplifications and examining the performance of the proposed model. Developed at Northwestern University with collaboration from the University of Amsterdam, the University Pablo de Olavide, and the University of Delft, RASPA code is mainly utilized in the area of thermodynamic properties of liquids and gases, and adsorption/diffusion behavior of adsorbates in crystalline nanoporous materials. The results generated by RASPA are considered to be high in correctness and accuracy because of the implementation of advanced techniques and algorithms, e.g., configurational-bias Monte Carlo (CBMC) and continuous fractional component Monte Carlo (CFCMC). Verified by data generated from experiments and RASPA 2.0 software, we will show that the model can accurately predict isotherms at different temperatures by using parameters fitted to one isotherm. We will also prove that the

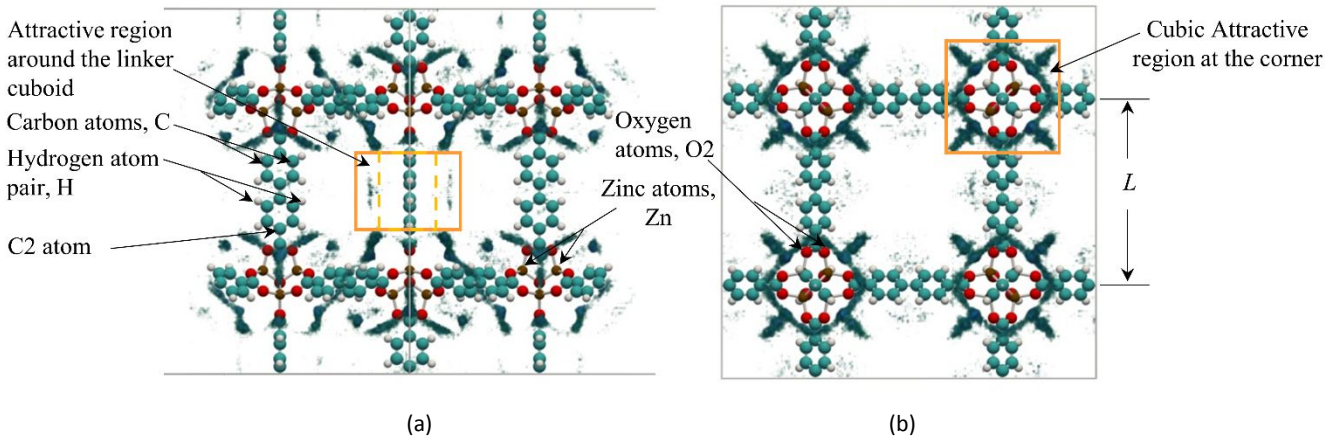

Fig. 2 Density distribution in the IRMOF-10 when 300 CH_4 molecules are assigned in the plotted structure space at 320 K

model also works for the adsorption prediction of quadrupolar gases, such as CO_2 and N_2.

2. Modeling

2.1 Simplified structure and attractive regions

In this section, we describe how we simplify the IRMOF structures, which will lead to the development of our engineering model. IRMOFs are cubic networks constructed by Zn_4O metal clusters and dicarboxylate linkers.[30] Due to their conformations, the shapes of void spaces in IRMOFs are irregular, and thus adsorption predictions based on models in cylindrical pores or slit pores are less reliable. We use RASPA 2.0 to generate data for the accessible surface of IRMOF-1 and visualize the results using the VTK software. Based on the shape of the accessible surface (Fig. 1(a)), we simplify the benzene ring and the ring formed by the dicarboxylate and the metal cluster to cuboids. The corner constructed by cuboids and the linker cuboid are shown in Fig. 1(b).

In the tiny space of the framework cell, both the metal atoms and the organic atoms of the frameworks generate attractive force. Thus, the force fields in the frameworks can be complicated, which makes it a tough task to build a simple engineering model for predicting the adsorption in IRMOFs, yet the distribution of the adsorbates inside the framework is not difficult to track. It has been observed that the adsorbed molecules tend to concentrate to the regions around the metal clusters first and then the regions around the linkers.[31,32] When the pressure is high enough, other concentrated regions of adsorbates will appear around the two concentrated regions mentioned above.[33] We track the locations of adsorbates during the simulation using RASPA 2.0 and present the density distribution (represented by the dark green cloud) in Fig. 2 when 300 methane molecules are assigned in the unit structure of IRMOF-10 at 320 K.

To build a simple model that can simplify the calculations, we further simplify the cuboids into square prisms (Fig. 1(c)) and roughly divide the void space into three regions, i.e., the cubic region around the corner with an evenly distributed attractive potential of $-\varepsilon_z$ (Fig. 1(d)), the region around the linker with an evenly distributed attractive potential of $-\varepsilon_b$ (Fig. 1(e)), and the middle region, which is not affected by the attractive force of the frameworks. Actually, the paddlewheel-fashion oriented linkers create cavities with two different sizes[34] where the densities of the adsorbates in those cavities are not the same. Since our model will calculate the average density in each attractive region that spans over other cells and cells of different sizes that exist periodically, it is not a necessity to discern the densities of different unit cells, and thus the simplified square prism linkers will be proven adequate.

Table 1 The dimension of the simplified structures[§]

	L	L_z	W_z_L	W_z_S	W_z	L_b	W_b_L	W_b_S	W_b
IRMOF-1	12.92					2.84			
IRMOF-10	17.14					7.06	5.2		3.5
IRMOF-16	21.49					11.41			
IRMOF-6	12.92	10.08	4.2	1.5	2.8	2.84	6.2	1.7	3.9
IRMOF-8	15.05					4.97	6.5		4.1
IRMOF-12	17.14					7.06	7.5		4.6
IRMOF-14	17.19					7.11	7.4		4.6

[§]Units: Å

The dimension of the simplified structure is determined by the real framework dimensions. According to Fig. 2, along the direction of the linkers, the concentration difference of the adsorbate on the upper and lower sides of the C2 atoms is noticeable. In fact, the same phenomenon also occurs in other IRMOFs. Therefore, we set the distance between the two C2 atoms on the linkers as the length of the linker prisms L_b. The side of the corner cube L_z is the difference between the side of the unit cell L and the linker length L_b. To calculate the widths of the square prisms, we firstly calculate the long widths and the short widths of the cuboids in Fig. 1(b), which shows the geometrical similarities to the real frameworks. Since the rings only have one layer of atoms, we set the average diameters of the atoms on the rings as the short widths (W_b_S, W_z_S) of the cuboids. For the long widths of the cuboids, we set the sum of the H atom diameter and the average distance of the H atoms pairs (Fig. 2) as the long widths (W_b_L, W_z_L). Because H atoms are small and they appear at the boundary of the benzene rings, they are not included in the calculation of the cuboids' short widths but are used for the calculation of the long widths. We then set the average values of the long widths (W_b_L, W_z_L) and the short widths (W_b_S, W_z_S) as the widths of the corresponding square prisms (W_b, W_z) in Fig. 1(c). Table 1 lists the parameters of IRMOFs mentioned in this paper, from which we can further conclude that the dimensions of the simplified structures are able to reflect the real materials, i.e., IRMOFs have the same corner clusters and the only difference of the linkers in IRMOF-1, IRMOF-10, and IRMOF-16 is the length.

2.2 Simulations for verifying the simplifications

Compared to the real conformations and properties of IRMOFs, the simplified structures and attractive regions provide us with a simple but clear understanding of the materials at the expense of ignoring the details and later enable us to develop the engineering model. However, it remains to be proven that the simplified structures could work well in generating isotherms that are in agreement with those obtained from experiments or from simulations using more realistic interaction potentials at atomistic level. To examine the applicability of the simplifications, we conduct GCMC simulations for the adsorption of methane in different IRMOFs using the simplified structures. Square-well potential is applied to represent the interactions among adsorbates and the interactions between adsorbates and IRMOFs. The parameters of adsorbates are from one version of the Statistical Associating Fluid Theory EOS (i.e., SAFT2[35]), the parameters of which are obtained by fitting the saturated pressure and saturated liquid density data.[36] These parameters can be found in Table 2, where ε represents the attractive potential among molecules, σ is the molecule diameter, $\lambda\sigma$ is the range of the potential well, and k is the Boltzmann constant. The interaction between the adsorbate molecule and the surface of adsorbent has the following expression:

$$u_{ms} = \begin{cases} +\infty & r_{mw} < \frac{1}{2}\sigma \\ -\varepsilon_z \; or \; -\varepsilon_b & \text{molecule center inside} \\ & attractive\ region \\ 0 & \text{molecule center outside} \\ & \text{attractive region } \& \; r_{mw} > \frac{1}{2}\sigma \end{cases} \quad (1)$$

where r_{mw} is the distance of the adsorbate molecule center to the surface of the simplified structure.

We assign at least 2 × 2 × 2 cells for the simulation box so that there are enough molecules to generate reliable results. Other simulation details can be found in our previous work.[37] Considering that there is only van der Waals interaction between a methane molecule and the structure atom, to keep the properties of the simplified structures consistent with the real materials, we assign the same attractive parameters to the clusters of the same conformations in different IRMOFs, i.e., we assign the same value of ε_z to the corner attractive regions of different IRMOFs and the same value of ε_b and δ for linkers' attractive regions of IRMOF-1, IRMOF-10, and IRMOF-16. Since the attractive parameters ε_z, ε_b, and δ are not available, we obtain them by fitting to realistic isotherms. The realistic isotherms are generated using RASPA 2.0 software. In this work, we choose the generic force field for the framework parameters, Transferable Potentials for Phase Equilibria (TraPPE) force field for adsorbate parameters, and Lennard-Jones (LJ) potential that is shifted to zero at the cutoff distance of 12Å with tail correction for the atomistic interactions.

Based on the description above, firstly, we fit the attractive parameters ε_z, ε_b, and δ for IRMOF-1, IRMOF-10, and IRMOF-16. Since they have the same conformations in linkers, i.e., benzene rings, and the only difference among these three frameworks are the linker length, their attractive parameters ε_z, ε_b, and δ are the same in our model. This step is consistent with the assumption that the clusters of the same conformations have the same attractive parameters. For the other IRMOFs, we only need to fit the two attractive parameters (ε_b, δ) for the linkers with the ε_z known from the first step. Table 3 lists the fitted parameters based on the isotherms generated by RASPA 2.0 at 250 K, which are then used for the adsorption predictions at various temperatures in this section. The precisions of the attractive potentials ε_z and ε_b are up to digit in the tens place and the width of the attractive region around the linkers δ is up to digit in the tenths place.

Table 2 Parameters of adsorbates from SAFT2 equation of state

	ε/k (K)	λ	σ (Å)
N_2	96.4703	1.5144	3.1942
CO_2	319.2744	1.3296	3.1788
CH_4	130.5206	1.5942	3.2968

Table 3 Simplified Simulation Parameters for CH_4 adsorption in different IRMOFs

	Corner	Linker	
	ε_z/k (K)	ε_b/k (K)	δ
IRMOF-1	940	690	0.3
IRMOF-10			
IRMOF-16			
IRMOF-6		590	0.4
IRMOF-8		620	0.4
IRMOF-12		560	0.6
IRMOF-14		550	0.6

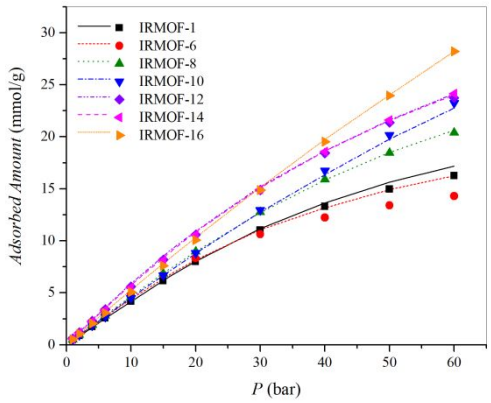

(a) CH_4 adsorption isotherms in different IRMOFs at 298 K.

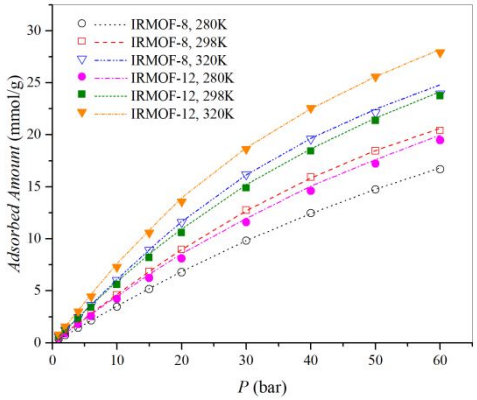

(b) CH_4 adsorption isotherms in IRMOF-8 and IRMOF-12 at different temperatures.

Fig. 3 Comparison of the isotherms generated by RASPA 2.0 (points) and the simulation using simplified structures (lines)

Fig. 3(a) presents the predicted isotherms for methane adsorption in different IRMOFs at 298 K. Fig. 3(b) presents the predicted isotherms for methane adsorptions in IRMOF-8 and IRMOF-12 at various temperatures. The good agreement of the predicted isotherms with those obtained using RASPA 2.0 software proves that the simplified structures and the defined attractive regions are able to reflect the adsorption phenomenon in the real case. Furthermore, compared with the real frameworks, the simplified structure uses simple prisms with flat surfaces to represents groups of the atoms. The complicated distribution of the adsorption sites analyzed by Dubbeldam et al.[33] is also replaced by simple attractive regions. Since these simplifications ignore the detailed locations of each atom on the framework and the detailed distribution of each adsorption site, the good performance of the model also suggests that adsorption isotherms are not sensitive to the detailed distribution of the attractive sites in the IRMOF structures and it is safe to ignore the geometrical details of the frameworks.

2.3 Theoretical model

The success of the application of square-well potential and the simplified structures makes it possible to build an engineering model for the prediction of the adsorption isotherms in IRMOFs. Since the system is regarded to be in equilibrium, the chemical potential of the adsorbed phase is equal to that of the bulk phase. To predict the adsorbed amount in the simplified structures, we equalize the chemical potentials of the adsorbate in each attractive region to that of the bulk phase. We have proven that in slit pores, the adsorbed amount in different attractive regions can be predicted independently regardless of the interactions among different regions.[37] For the density in the middle region, which is not influenced by the attractive force of the framework, we approximate it using the density in the bulk. The chemical potential and density of the bulk phase are calculated using SAFT2.

The expression of the chemical potential of the fluid in the attractive region is derived from the generalized van der Waals canonical partition function *Q(T, V, N)*, as given below:[37]

$$Q(T,V,N) = \left(\frac{q_{int}^N}{\Lambda^{3N}N!}\right)V_f^N \exp\left(\int_\infty^T \frac{E_{conf}}{kT^2}dT\right) \quad (2)$$

$$\mu = -kT\left[\frac{\partial \ln(Q)}{\partial N}\right]_{T,V} \quad (3)$$

where T is the temperature, V is the volume, N is the number of molecules, q_{int} is the internal energy partition function for one molecule, Λ is the de Broglie wavelength of the molecules, V_f is the free volume of the hard-core fluid, E_{conf} is the configurational energy, and μ is the chemical potential. According to the generalized van der Waals canonical partition function and the expression for the chemical potential, two key quantities for the calculation of the chemical potential in the different attractive regions are free volume and configurational energy.

The free volume in a certain attractive region is expressed as follows:

$$V_f = V - \frac{N}{\rho_{max}} \quad (4)$$

where ρ_{max} is the close-packed density of adsorbates in the attractive region. Since the packing effects are expected to be insignificant in real IRMOFs because the interaction with the pore structure is not strongly felt throughout the space of the frameworks,[38] the close-packed density is approximated by that of the bulk, i.e., $\sqrt{2}$.

Since each cell in the IRMOF structure is tiny, it is unavoidable that different attractive regions overlap, which could lead to more complicated calculations. Because of the features of the simplified structure and attractive regions, only the linkers' attractive regions could overlap. The configurational energy in a certain non-overlapping or overlapping attractive region is given by:

$$E_{conf} = -\frac{N}{2}N_c\varepsilon - nN\varepsilon_s \quad (5)$$

where the first term is to account for the energy generated by the interaction among adsorbates and the second term is to account for the energy from adsorbate-structure interaction in the region. In Equation (5), N_c is the coordination number, ε_s is

the attractive potential of the adsorbate-structure interaction (ε_b or ε_z), and n is the number of attractive potentials of the adsorbate-structure interaction affecting the region. For a non-overlapping region, the value of n is 1. In this work, we control the sizes of the linkers' attractive regions (δ) and limit them such that triple or quadruple overlaps will not happen, and thus the maximum value of n is 2. By doing this, we can avoid the complex analysis regarding the shape of the regions with triple or quadruple overlaps and the calculation becomes simpler. The distribution of the attractive regions and the occurrence of overlaps are depicted and explained in the supplementary material. As shown later, although triple overlaps are avoided, the isotherms obtained from both the simplified simulation and the modeling are still in agreement with those obtained from RASPA 2.0.

By assuming uniform density in each region, the coordination number of a region can be obtained from:

$$N_c = 4\pi\rho\int g(r,\rho,T)r^2dr \quad (6)$$

where g is the radial distribution function and ρ is the number density in the region. As in our previous work,[37] the radial distribution function used in the derivation of the coordination number is approximated by the low-density radial distribution function for square-well fluid, i.e., $g(r, \rho = 0, T)$:

$$g(r) = \begin{cases} 0 & r < \sigma \\ exp\left(\frac{\varepsilon}{kT}\right) & \sigma \le r \le \lambda\sigma \\ 1 & r > \lambda\sigma \end{cases} \quad (7)$$

where r is the center to center distance between the central molecule and the molecule around it.

The expression of the coordination number was shown to simplify to:[37]

$$N_c = Cexp\left(\frac{\varepsilon}{kT}\right)\rho^* \quad (8)$$

where C represents the reduced volume of the potential well of a molecule within the attractive region and ρ^* is the reduced density ($=\rho\sigma^3$). Unlike the prediction of the coordination number for molecules in slit pores, the reduced volume C is no longer a constant at different locations in each attractive region of the simplified IRMOF structure. However, since the volume of each attractive region is small, we set C to be a constant and will check in this section if high accuracy of isotherm prediction can still be achieved. Since the range of δ is controlled such that triple overlaps will not happen, the volume of the overlapped regions could be even smaller than that of a methane molecule in some frameworks. Thus, we can safely set the reduced volume constant in these regions to zero, which means we neglect the existence of adsorbate-adsorbate interaction in the overlapping regions.

From the above analysis, the expression of the chemical potential of an attractive region is:

$$\mu = RT\left[ln\left(\frac{\Lambda^3 N_{av}}{v-b}\right) + \frac{b}{v-b}\right] - \frac{2a}{v} - N_{av}n\varepsilon_s \quad (9)$$

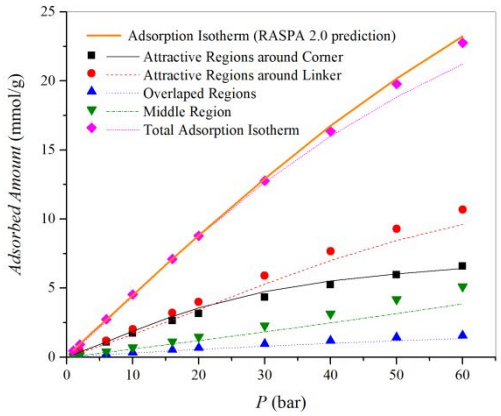

points are obtained from simplified simulation; lines are model prediction

Fig. 4 Adsorbed amounts of methane in different regions for IRMOF-10 at 298 K

where N_{av} is the Avogadro number, R is the gas constant ($= kN_{av}$), v is the molar volume in the region, and a and b are the van der Waals parameters in our model given by:

$$a = N_{av}^2\frac{C\sigma}{2}kT\left[exp\left(\frac{\varepsilon}{kT}\right) - 1\right] \quad (10)$$

$$b = \frac{N_{av}}{\rho_{max}} \quad (11)$$

In Equation (10), $C = C_z$ for the attractive region at the corner, $C = C_b$ for the non-overlapping attractive region around linker, and $C = 0$ for the overlapping linkers' attractive region.

To check the applicability of constant reduced volumes, in this section we directly fit the reduced volume constants in non-overlapping attractive regions using the densities in those regions obtained from simplified simulation at one temperature and apply them to predict the adsorbed amounts at other temperatures. Fig. 4 presents the predicted adsorbed amounts of CH_4 in different regions of IRMOF-10 and the overall performance of the model in predicting isotherms at 298 K by using the reduced volumes fitted from the densities of the attractive regions at 250 K and the other parameters from Table 3. It is noticeable that the underestimation of the overall adsorbed amount at high pressure is mainly because of the underestimation of the density in the middle region, where the density is assumed to be the same as that in the bulk phase. In real case, when the pressure is high, the density in the middle region starts to deviate from that of the bulk phase. Nevertheless, we still can conclude that the model works well in predicting the densities in attractive regions, and the reduced volume constants fitted from the isotherm at one temperature can be applied to the prediction of isotherms at other temperatures. The error at high pressures will be fixed and explained in the next section.

3. Results and Applications

The previous sections indicate that the model can predict the densities of different attractive regions by fitting the reduced volumes. However, it would be a time-consuming process if we obtain the five parameters (ε_z, ε_b, δ, C_z, C_b) by conducting

simplified simulations. In fact, we can obtain all the parameters by directly fitting the model to real isotherms.

Table 4. The predicted adsorbed amounts of different adsorbates in different IRMOFs are in good agreements with the

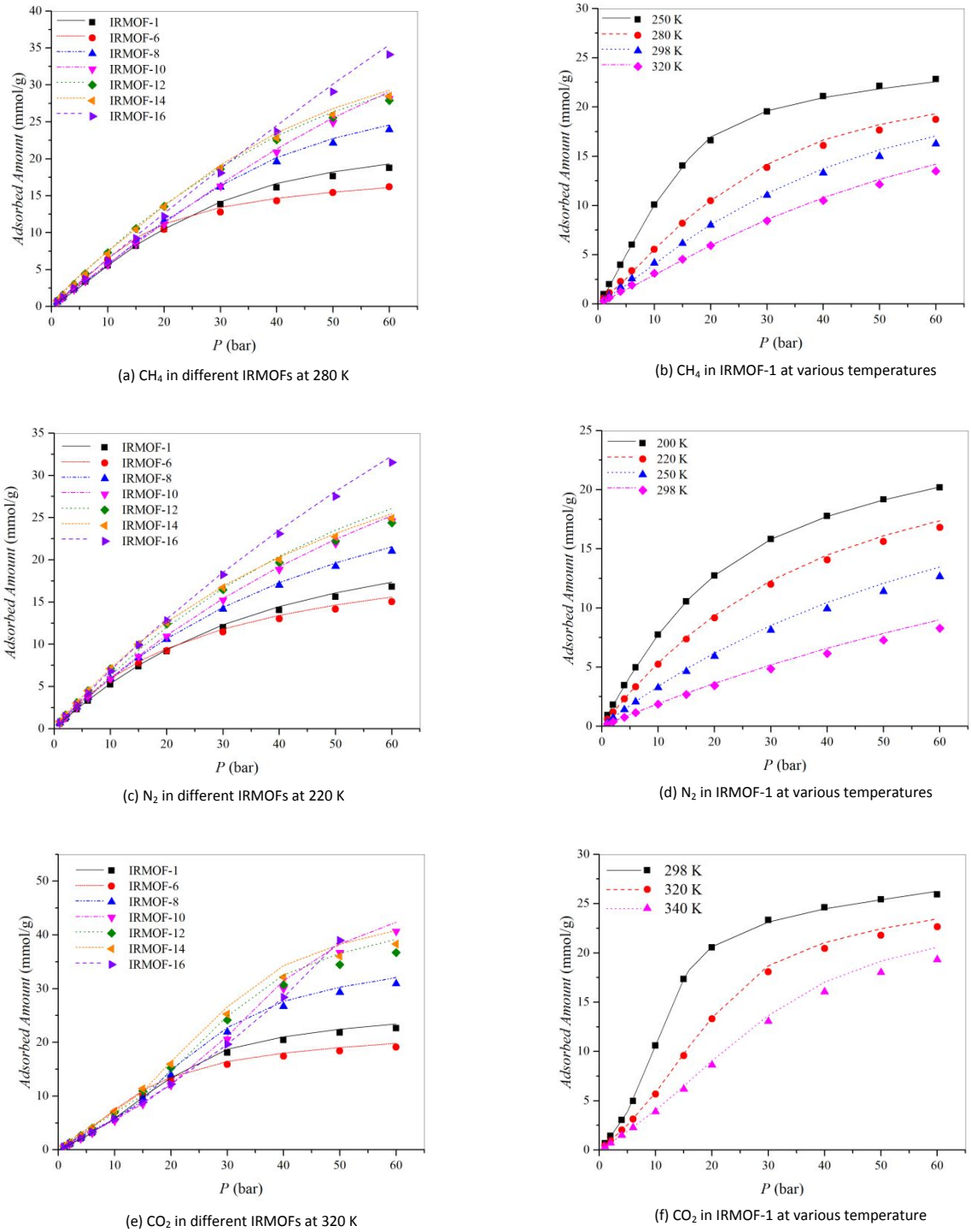

(a) CH_4 in different IRMOFs at 280 K

(b) CH_4 in IRMOF-1 at various temperatures

(c) N_2 in different IRMOFs at 220 K

(d) N_2 in IRMOF-1 at various temperatures

(e) CO_2 in different IRMOFs at 320 K

(f) CO_2 in IRMOF-1 at various temperature

Fig. 5 Adsorption isotherms obtained from RASPA 2.0 (points) and the model prediction (lines)

Figs. 5(a) and 5(b) are the predicted isotherms of CH_4 based on the parameters fitted to the isotherms at 250 K, Figs. 5(c) and 5(d) are the predicted isotherms of N_2 based on the parameters fitted to the isotherms at 200 K, and Figs. 5(e) and 5(f) are the predicted isotherms of CO_2 based on the parameters fitted to the isotherms at 298 K. These parameters are listed in data generated by RASPA 2.0, and the different types of isotherms (IUPAC adsorption Type I and Type V) [39] are well captured.

For quadrupolar gases, such as N_2 and CO_2, the interactions between the adsorbate and IRMOFs are not only van der Waals interaction, but also Coulombic interactions, which play an

important role because of the partial charges of the IRMOF atoms. The influence of Coulombic interactions, in a macroscopic point of view, is evident from the high densities of adsorbates around the corner and linker. Therefore, this will not influence the implementation of the model since the distribution of the quadrupolar molecules inside the structures is similar to that of non-polar adsorbates,33 which means that predicting the isotherms can still be achieved by predicting the adsorbed amount in each attractive region. In other words, the influence of the Coulombic interaction does not need additional treatment and the model, which only considers square-well potentials, works as well as it does for non-polar molecules. No additional parameters or model modifications are needed.

From Fig. 5, we find that the predicted isotherms are in agreement with the results obtained from RASPA 2.0. This fact further confirms that the fitted attractive parameters absorb the influence of the interactions among different attractive regions. For comparison, predictions of methane adsorption in IRMOF-6 and IRMOF-8 at 298 K have been attempted using SL and PHSC EOS,[26] but the results were found to be unsatisfactory.

As mentioned at the beginning of this paper, for the same kind of materials, the isotherm at the same temperature can vary if the materials are synthesized by different research groups. Although the interaction potential used in doing molecular simulation is close to the real value, errors still exist when compared with the experimental data, because materials synthesized in the lab are not as ideal as that in the simulation and the purity of the materials are different to a certain degree due to different experimental conditions. Therefore, if we want to predict the isotherms of a material synthesized in a particular lab, doing molecular simulation or using adsorption models with parameters obtained from data of other labs/experiments will not be able to accurately predict its isotherms. The model proposed in this work just needs an isotherm at one temperature to find the parameters, and the isotherms at other temperatures can be predicted accurately. Fig. 6 presents the performance of our model in predicting isotherms. The scattered points are the experimental data.[40] For the adsorption of CH_4 in IRMOF-1, which have lower values than those obtained from RASPA 2.0, and are very different from those obtained in other experimental works.[41,42] We fitted the five parameters in our model to the isotherm at 248.5 K (ε_z/k = 921.1 K , ε_b/k = 574.1 K, δ = 0.35, C_z = 4.0, C_b = 5.1) and use this set of parameters to predict the isotherms at other temperatures. The excellent agreement with the experimental data demonstrates that our model can be a powerful tool for predicting the isotherms of real materials.

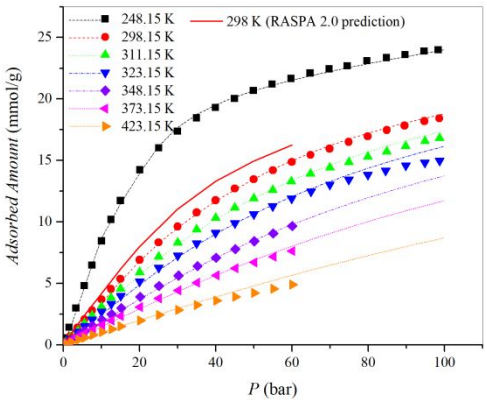

Fig. 6 Experimental isotherms (points) and predicted isotherms (lines) for CH_4 adsorption in IRMOF-1

Table 4 Fitted Parameters for CH_4, CO_2, and N_2 adsorption in different IRMOFs

		ε_z/k (K)	ε_b/k (K)	δ	C_z	C_b
CH_4	IRMOF-1	956.2	642.5	0.35	4.14	5.40
	IRMOF-6	828.0	1017.0	0.29	4.88	4.68
	IRMOF-8	857.0	637.2	0.49	5.03	5.08
	IRMOF-10	799.7	573.5	0.60	3.87	4.32
	IRMOF-12	860.1	654.5	0.61	5.00	4.37
	IRMOF-14	736.5	666.0	0.62	5.50	4.21
	IRMOF-16	707.1	472.5	0.79	4.13	3.83
CO_2	IRMOF-1	1070.0	835.0	0.36	1.79	2.16
	IRMOF-6	1163.0	986.3	0.37	1.71	1.79
	IRMOF-8	834.2	784.5	0.56	2.49	2.10
	IRMOF-10	846.8	684.7	0.63	2.20	1.99
	IRMOF-12	835.9	759.7	0.66	2.49	2.12
	IRMOF-14	828.2	756.8	0.68	2.52	2.15
	IRMOF-16	918.8	610.0	0.62	1.67	2.20
N_2	IRMOF-1	741.2	559.5	0.31	2.11	3.80
	IRMOF-6	838.4	608.9	0.31	2.10	3.30
	IRMOF-8	707.0	510.8	0.44	3.28	3.49
	IRMOF-10	685.1	475.4	0.45	2.03	3.17
	IRMOF-12	728.2	517.3	0.49	4.21	3.32
	IRMOF-14	714.9	509.3	0.50	4.32	3.37
	IRMOF-16	668.5	436.7	0.51	1.62	2.76

4. Conclusions

A simple engineering model for adsorption derived from the Generalized van der Waals partition function is proposed to describe the isotherms of light gas adsorption in IRMOFs. The model is developed by making reasonable simplification to the structures of IRMOFs and defining important attractive regions of square-well potential. The simplification of the structures is based on the geometries of the accessible surfaces and the dimensions of the frameworks. The locations of the attractive regions are defined by examining the distribution of the concentrated adsorbates.

The reliability of the simplification is first verified by conducting molecular simulations. Grand Canonical Monte Carlo (GCMC) simulations using both the simplified structures with square-well potentials and the complete atomic structures with Lennard-Jones and Coulombic potentials are performed and compared. Simulations based on Lennard-Jones potential are conducted as a reference to the simplified simulation and the adsorption model. We demonstrate that the simplified simulation can generate the adsorption isotherms of different IRMOFs with high accuracy and the model can predict the adsorbed amounts in different attractive regions accurately. Given one of the isotherms, we can fit the five parameters of the model and use them to accurately predict the isotherms at other temperatures. For the adsorption of quadrupolar molecules, the effect of the columbic interactions can be adsorbed by the square-well potential and the adsorption isotherms in IRMOFs can still be predicted accurately.

It is also demonstrated that the application of the model is not limited to the adsorption prediction in ideal IRMOF structures, i.e., the structures used in simulations, but also in frameworks synthesized by experiments, which are imperfect in purity and structure completeness. The predicted isotherms using our model can accurately match those obtained from experiments.

Conflicts of interest

There are no conflicts to declare.

Acknowledgements

This work is supported by the State of Wyoming and the Department of Energy (DE-PI0000017).

References

1 A. U. Czaja, N. Trukhan and U. Muller, *Chemical Society Reviews*, 2009, **38**, 1284-1293.
2 J. R. Li, R. J. Kuppler and H. C. Zhou, *Chemical Society Reviews*, 2009, **38**, 1477-1504.
3 T. Duren, Y. S. Bae and R. Q. Snurr, *Chemical Society Reviews*, 2009, **38**, 1237-1247.
4 R. B. Getman, Y. S. Bae, C. E. Wilmer and R. Q. Snurr, *Chemical Reviews*, 2012, **112**, 703-723.
5 A. K. Rappe, C. J. Casewit, K. S. Colwell, W. A. Goddard and W. M. Skiff, *Journal of the American Chemical Society*, 1992, **114**, 10024-10035.
6 S. L. Mayo, B. D. Olafson and W. A. Goddard, *Journal of Physical Chemistry*, 1990, **94**, 8897-8909.
7 S. Amirjalayer and R. Schmid, *Journal of Physical Chemistry C*, 2008, **112**, 14980-14987.
8 L. C. Lin, K. Lee, L. Gagliardi, J. B. Neaton and B. Smit, *Journal of Chemical Theory and Computation*, 2014, **10**, 1477-1488.
9 O. Engkvist, P. O. Astrand and G. Karlstrom, *Chemical Reviews*, 2000, **100**, 4087-4108.
10 T. Mueller and G. Ceder, *Journal of Physical Chemistry B*, 2005, **109**, 17974-17983.
11 A. L. Dzubak, L. C. Lin, J. Kim, J. A. Swisher, R. Poloni, S. N. Maximoff, B. Smit and L. Gagliardi, *Nature Chemistry*, 2012, **4**, 810-816.
12 P. L. Liao, R. B. Getman and R. Q. Snurr, *Acs Applied Materials & Interfaces*, 2017, **9**, 33484-33492.
13 L. J. Chen, C. A. Morrison and T. Duren, *Journal of Physical Chemistry C*, 2012, **116**, 18899-18909.
14 C. E. Wilmer, M. Leaf, C. Y. Lee, O. K. Farha, B. G. Hauser, J. T. Hupp and R. Q. Snurr, *Nature Chemistry*, 2012, **4**, 83-89.
15 C. Altintas and S. Keskin, *Chemical Engineering Science*, 2016, **139**, 49-60.
16 E. Haldoupis, S. Nair and D. S. Sholl, *Journal of the American Chemical Society*, 2012, **134**, 4313-4323.
17 R. Krishna, *Rsc Advances*, 2017, **7**, 35724-35737.
18 Z. W. Qiao, Q. S. Xu, A. K. Cheetham and J. W. Jiang, *Journal of Physical Chemistry C*, 2017, **121**, 22208-22215.
19 H. Frost, T. Duren and R. Q. Snurr, *Journal of Physical Chemistry B*, 2006, **110**, 9565-9570.
20 J. L. Mendoza-Cortes, S. S. Han, H. Furukawa, O. M. Yaghi and W. A. Goddard, *Journal of Physical Chemistry A*, 2010, **114**, 10824-10833.
21 H. D. Zhang, P. Deria, O. K. Farha, J. T. Hupp and R. Q. Snurr, *Energy & Environmental Science*, 2015, **8**, 1501-1510.
22 K. Sillar, A. Hofmann and J. Sauer, *Journal of the American Chemical Society*, 2009, **131**, 4143-4150.
23 K. Sillar and J. Sauer, *Journal of the American Chemical Society*, 2012, **134**, 18354-18365.
24 S. J. Alesaadi and F. Sabzi, *International Journal of Hydrogen Energy*, 2014, **39**, 21076-21082.
25 S. J. Alesaadi and F. Sabzi, *International Journal of Hydrogen Energy*, 2014, **39**, 14851-14857.
26 M. Tahmooresi and F. Sabzi, *Journal of Inorganic and Organometallic Polymers and Materials*, 2015, **25**, 1298-1304.
27 V. M. Trejos, A. Martinez and A. Gil-Villegas, *Fluid Phase Equilibria*, 2018, **462**, 153-171.
28 M. Eddaoudi, J. Kim, N. Rosi, D. Vodak, J. Wachter, M. O'Keeffe and O. M. Yaghi, *Science*, 2002, **295**, 469–472.
29 D. Dubbeldam, S. Calero, D. E. Ellis and R. Q. Snurr, *Molecular Simulation*, 2016, **42**, 81-101.
30 D. Fairen-Jimenez, N. A. Seaton and T. Duren, *Langmuir*, 2010, **26**, 14694-14699.
31 Q. T. Ma, Q. Y. Yang, C. L. Zhong, J. G. Mi and D. H. Liu, *Langmuir*, 2010, **26**, 5160-5166.
32 N. S. Suraweera, R. C. Xiong, J. P. Luna, D. M. Nicholson and D. J. Keffer, *Molecular Simulation*, 2011, **37**, 621-639.
33 D. Dubbeldam, H. Frost, K. S. Walton and R. Q. Snurr, *Fluid Phase Equilibria*, 2007, **261**, 152-161.
34 T. Duren, L. Sarkisov, O. M. Yaghi and R. Q. Snurr, *Langmuir*, 2004, **20**, 2683-2689.
35 S. P. Tan, X. Y. Ji, H. Adidharma and M. Radosz, *Journal of Physical Chemistry B*, 2006, **110**, 16694-16699.
36 NIST Chemistry Webbook,

http://www.webbook.nist.gov/chemistry/, (accessed July 2018).
37 L. L. Kong and H. Adidharma, *Chemical Engineering Science*, 2018, **177**, 323-332.
38 T. Duren and R. Q. Snurr, *Journal of Physical Chemistry B*, 2004, **108**, 15703-15708.
39 K. S. W. Sing, D. H. Everett, R. A. W. Haul, L. Moscou, R. A. Pierotti, J. Rouquerol and T. Siemieniewska, *Pure and Applied Chemistry*, 1985, **57**, 603-619.
40 J. A. Mason, M. Veenstra and J. R. Long, *Chemical Science*, 2014, **5**, 32-51.
41 D. Saha, Z. B. Bao, F. Jia and S. G. Deng, *Environmental Science & Technology*, 2010, **44**, 1820-1826.
42 W. Zhou, H. Wu, M. R. Hartman and T. Yildirim, *Journal of Physical Chemistry C*, 2007, **111**, 16131-16137.